IEEE Access
Multidisciplinary | Rapid Review | Open Access Journal

Received October 15, 2020, accepted October 31, 2020, date of publication November 6, 2020, date of current version November 19, 2020.

Digital Object Identifier 10.1109/ACCESS.2020.3036401

Phase Shift Adjustable Pilots for Channel Acquisition in Vehicle-to-Vehicle Underlay Wideband Massive MIMO

XINXIN NIU, (Student Member, IEEE), LI YOU, (Member, IEEE), AND XIQI GAO, (Fellow, IEEE)

National Mobile Communications Research Laboratory, Southeast University, Nanjing 210096, China
Purple Mountain Laboratories, Nanjing 211100, China

Corresponding author: Xiqi Gao (xqgao@seu.edu.cn)

This work was supported in part by the National Key Research and Development Program of China under Grant 2018YFB1801103; in part by the National Natural Science Foundation of China under Grant 61801114, Grant 61761136016, and Grant 61631018; in part by the Jiangsu Province Basic Research Project under Grant BK20192002; and in part by the Huawei Cooperation Project.

ABSTRACT Decrease of the pilot overhead is an important issue in vehicle-to-vehicle (V2V) underlay wideband massive multiple-input multiple-output (mMIMO) communication. To reduce the pilot overhead for channel acquisition, we propose phase shift adjustable pilots (PSAPs) for V2V underlay wideband mMIMO systems employing orthogonal frequency division multiplexing (OFDM). Motivated by the sparse property of the angle-delay (AD) domain channels in mMIMO, we first investigate channel acquisition for V2V underlay mMIMO-OFDM with PSAPs, and derive the optimal conditions to achieve the sum mean square error (sMSE) minimums of channel estimation and channel prediction, respectively. The optimal conditions indicate that the minimum sMSE can be achieved when the AD domain channel power spectra of cellular users (CUs) and transmitters in V2V communication pairs are non-overlapping after appropriate allocation of the available pilot phase shifts. Then an AD domain channel power spectrum based pilot allocation (ADCPS-PA)algorithm is developed according to the optimal conditions. Simulation results indicate that the achievable spectral efficiency for both cellular and V2V links can be significantly improved with PSAPs compared with that obtained by the conventional phase shift orthogonal pilot approach.

INDEX TERMS Channel acquisition, phase shift adjustable pilots, pilot phase shift allocation, V2V underlay, wideband massive MIMO.

I. INTRODUCTION

With the arrival of 5G wireless communication, vehicle-to-vehicle (V2V) communication has gained significant research interest for its potential in intelligent automotive and transportation industries. Compared to the vehicular communication introduced by 802.11p, the cellular based vehicle-to-everything proposed by 3GPP can achieve lower latency, higher data rates, and longer transmission ranges [1]. In cellular based V2V communication, spectrum can be shared by means of the overlay or underlay schemes among cellular and V2V users [2]. In the overlay scheme, separate frequency bands are allocated to V2V and cellular transmission, which protects cellular users (CUs) but may decrease the spectral efficiency in some cases. Whereas in the underlay scheme, all the users in cellular and V2V links can use the same spectrum resources in the mean while, which improves the spectrum utilization. Because of the growing demand for high data rates, massive multiple-input multiple-output (mMIMO), which can provide high efficiency in spectral and energy utilization, is envisioned as an attractive technology for future V2V communication [3]. Particularly, it has been suggested that V2V underlay mMIMO transmission is one of the promising technologies for future 5G communication networks [4], [5].

Orthogonal frequency division multiplexing (OFDM) is suited for wideband mMIMO communication, and channel acquisition plays an important role in mMIMO-OFDM systems. In the conventional orthogonal pilot approach to acquire channel state information (CSI), the channel response is estimated in the delay domain and the phase shifts of pilots for different transmit antennas need to satisfy the

The associate editor coordinating the review of this manuscript and approving it for publication was Christoph Studer.

TABLE 1. List of notations.

$\mathbf{I}_N$	the N-dimensional identity matrix
$\mathbf{I}_{N\times G}$	the matrix comprised of the first $G\,(\leq N)$ columns of $\mathbf{I}_N$
$\mathbf{F}_N$	the N-dimensional unitary discrete Fourier transform matrix
$\mathbf{F}_{N\times G}$	the matrix comprised of the first $G\,(\leq N)$ columns of $\mathbf{F}_N$
$\mathbf{f}_{N,m}$	the mth column of $\sqrt{N}\mathbf{F}_N$
$\mathrm{diag}\,\{\mathbf{x}\}$	the diagonal matrix with vector $\mathbf{x}$ along its main diagonal
$\mathsf{vec}\,\{\cdot\}$	the vectorization operation
$\langle\cdot\rangle_N$	the modulo-N operation
$\mathbf{\Pi}_N^m$	the permutation matrix which is defined as $\mathbf{\Pi}_N^m \triangleq \begin{bmatrix} \mathbf{0} & \mathbf{I}_{N-\langle m\rangle_N} \\ \mathbf{I}_{\langle m\rangle_N} & \mathbf{0} \end{bmatrix}$

orthogonality condition [6]. However, such phase shift orthogonal pilots (PSOPs) do not take the pilot overhead issue into consideration. Note that due to high mobility and fast V2V channel fading, channel acquisition might need to be performed more frequently in V2V underlay mMIMO-OFDM transmission, which leads to more pilot overhead and reduced system performance. Thus, the pilot overhead is considered as one of the bottlenecks in practical V2V underlay mMIMO-OFDM systems.

To decrease the pilot overhead, non-orthogonal pilots have obtained much research interest in recent years. [7]–[9] investigate non-orthogonal pilot approaches in the simple cellular user scenarios, based on the channel sparsity in the angle domain. [10] proposes a strategy where orthogonal pilots are assigned to cellular users while V2V links reuse another set of pilots. Further more, [11] and [12] expand pilot reuse to all the cellular and V2V users over the frequency-flat channels.

In this work, phase shift adjustable pilots (PSAPs) are proposed for V2V underlay mMIMO-OFDM transmission. Unlike conventional PSOPs, the phase shifts of different pilots in our proposed approach are adjustable and can be less than the maximum channel delay. Thus, more available pilots can be utilized to serve the increasing users, and significant reduction for the pilot overhead can be achieved. Based on the angle-delay (AD) domain channel sparsity [8], we first investigate channel acquisition for V2V underlay mMIMO-OFDM with PSAPs, and derive the optimal conditions under which the sum mean square error (sMSE) for channel estimation (CE) and channel prediction (CP) can be minimized, respectively. The optimal conditions indicate that the minimum sMSE can be achieved when the AD domain channel power spectra (CPS) of different CUs and transmitters in V2V communication pairs become non-overlapping with proper pilot phase shift allocation. Then an AD domain CPS based pilot allocation (ADCPS-PA) algorithm is developed based on the optimal conditions. Simulations show that the proposed PSAP approach can dramatically improve the spectral efficiency performance for both CUs and V2V links, compared with the conventional PSOP approach.

Notations and acronyms used throughout this paper and their explanations are detailed in Table 1 and Table 2, respectively.

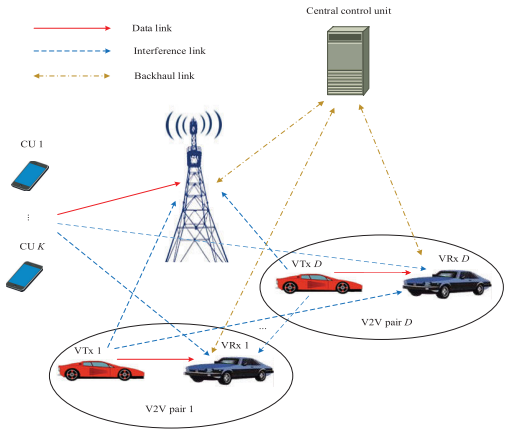

FIGURE 1. The single-cell V2V underlay mMIMO wireless communication.

II. WIDEBAND mMIMO CHANNEL MODEL

Consider the single-cell V2V underlay wideband mMIMO wireless communication in the TDD mode, which consists of one M-antenna base station (BS), K single-antenna CUs, and D V2V communication pairs, illustrated in Fig. 1. The dth V2V communication pair includes a single-antenna transmitter (VTx) and a N_d-antenna receiver (VRx). We denote the sets of CUs, VTxs, VRxs as $\mathcal{K}$, $\mathcal{V}_{\mathrm{Tx}}$, and $\mathcal{V}_{\mathrm{Rx}}$, respectively. Assume that the channels of different CUs and VTxs of V2V communication pairs are statistically independent.

OFDM modulation with N_{c} subcarriers is considered, and the guard interval $T_{\mathrm{g}} = N_{\mathrm{g}}T_{\mathrm{s}}$ is assumed to be not less than the maximum channel delay of all the users, where N_{g} $(\leq N_{\mathrm{c}})$ is the cyclic prefix length and T_{s} is the system sampling duration.

Assume that the channels remain constant for a symbol duration, and vary from symbol to symbol. Denote by $\mathbf{g}^{\mathrm{cb}}_{k,\ell,n}$, $\mathbf{g}^{\mathrm{vb}}_{i,\ell,n}$, $\mathbf{g}^{\mathrm{cv}}_{k,d,\ell,n}$, and $\mathbf{g}^{\mathrm{vv}}_{i,d,\ell,n}$ the channel vectors from the kth CU to the BS, the ith VTx to the BS, the kth CU to the dth VRx, and the ith VTx to the dth VRx over OFDM symbol ℓ and subcarrier n, respectively. Then we denote the channels from the kth CU to the BS, the ith VTx to the BS, the kth CU to the dth VRx, and the ith VTx to the dth VRx over all

TABLE 2. List of acronyms.

AD	angle-delay
ADCPM	AD domain channel power matrix
ADCPS-PA	AD domain channel power spectrum based pilot allocation
ADCRM	AD domain channel response matrix
AWGN	additive white Gaussian noise
BS	base station
CE	channel estimation
CP	channel prediction
CPS	channel power spectra
CSI	channel state information
CU	cellular user
i.i.d.	identically and independently distributed
mMIMO	massive MIMO
MMSE	minimum mean square error
OFDM	orthogonal frequency division multiplexing
PI	pilot interference
PSAP	phase shift adjustable pilot
PSOP	phase shift orthogonal pilot
SF	space-frequency
sMSE	sum mean square error
TCF	temporal correlation function
V2V	vehicle-to-vehicle
VRx	receiver in the V2V communication pair
VTx	transmitter in the V2V communication pair

subcarriers at OFDM symbol ℓ by

$$\begin{aligned}
\mathbf{G}^{\mathrm{cb}}_{k,\ell} &= \left[\mathbf{g}^{\mathrm{cb}}_{k,\ell,0} \quad \mathbf{g}^{\mathrm{cb}}_{k,\ell,1} \quad \cdots \quad \mathbf{g}^{\mathrm{cb}}_{k,\ell,N_{\mathrm{c}}-1}\right] \in \mathbb{C}^{M\times N_{\mathrm{c}}},\\
\mathbf{G}^{\mathrm{vb}}_{i,\ell} &= \left[\mathbf{g}^{\mathrm{vb}}_{i,\ell,0} \quad \mathbf{g}^{\mathrm{vb}}_{i,\ell,1} \quad \cdots \quad \mathbf{g}^{\mathrm{vb}}_{i,\ell,N_{\mathrm{c}}-1}\right] \in \mathbb{C}^{M\times N_{\mathrm{c}}},\\
\mathbf{G}^{\mathrm{cv}}_{k,d,\ell} &= \left[\mathbf{g}^{\mathrm{cv}}_{k,d,\ell,0} \quad \mathbf{g}^{\mathrm{cv}}_{k,d,\ell,1} \quad \cdots \quad \mathbf{g}^{\mathrm{cv}}_{k,d,\ell,N_{\mathrm{c}}-1}\right] \in \mathbb{C}^{N_d\times N_{\mathrm{c}}},\\
\mathbf{G}^{\mathrm{vv}}_{i,d,\ell} &= \left[\mathbf{g}^{\mathrm{vv}}_{i,d,\ell,0} \quad \mathbf{g}^{\mathrm{vv}}_{i,d,\ell,1} \quad \cdots \quad \mathbf{g}^{\mathrm{vv}}_{i,d,\ell,N_{\mathrm{c}}-1}\right] \in \mathbb{C}^{N_d\times N_{\mathrm{c}}},
\end{aligned} \tag{1}$$

respectively.

Assume that the temporal correlations and joint space-frequency (SF) domain correlations for the channels can be separated, and channels with different incidence angles, delays, and Doppler frequencies are uncorrelated, then we can obtain the following channel statistical property [8]

$$\begin{aligned}
\mathrm{E}\left\{\mathrm{vec}\left\{\mathbf{G}^{\mathrm{xb}}_{k,\ell+\Delta_\ell}\right\}\mathrm{vec}^H\left\{\mathbf{G}^{\mathrm{xb}}_{k,\ell}\right\}\right\} &= \tau^{\mathrm{xb}}_k(\Delta_\ell)\cdot\mathbf{R}^{\mathrm{xb}}_k,\\
\mathrm{E}\left\{\mathrm{vec}\left\{\mathbf{G}^{\mathrm{xv}}_{k,d,\ell+\Delta_\ell}\right\}\mathrm{vec}^H\left\{\mathbf{G}^{\mathrm{xv}}_{k,d,\ell}\right\}\right\} &= \tau^{\mathrm{xv}}_{k,d}(\Delta_\ell)\cdot\mathbf{R}^{\mathrm{xv}}_{k,d},
\end{aligned} \tag{2}$$

for $\mathrm{x}\in\{\mathrm{c},\mathrm{v}\}$, where τ^{xb}_k and $\tau^{\mathrm{xv}}_{k,d}$ are the corresponding channel temporal correlation functions (TCFs) from one CU or VTx to the BS and the dth VRx, respectively, and $\mathbf{R}^{\mathrm{xb}}_k\in\mathbb{C}^{MN_{\mathrm{c}}\times MN_{\mathrm{c}}}$ and $\mathbf{R}^{\mathrm{xv}}_{k,d}\in\mathbb{C}^{N_dN_{\mathrm{c}}\times N_dN_{\mathrm{c}}}$ are the corresponding SF domain channel covariance matrices. The channel elements for different links are assumed to be jointly Gaussian distributed, i.e., $\mathrm{vec}\left\{\mathbf{G}^{\mathrm{xb}}_{k,\ell}\right\}\sim\mathcal{CN}\left(\mathbf{0},\mathbf{R}^{\mathrm{xb}}_k\right)$ and $\mathrm{vec}\left\{\mathbf{G}^{\mathrm{xv}}_{k,d,\ell}\right\}\sim\mathcal{CN}\left(\mathbf{0},\mathbf{R}^{\mathrm{xv}}_{k,d}\right)$ via the law of large numbers.

It has been shown in [8] that when M and N_d are sufficiently large, a remarkably good approximation for the SF domain channel covariance matrices can be obtained, shown as follows

$$\begin{aligned}
\mathbf{R}^{\mathrm{xb}}_k &\approx \beta^{\mathrm{xb}}_k\left(\mathbf{F}_{N_{\mathrm{c}}\times N_{\mathrm{g}}}\otimes\mathbf{V}_M\right)\mathrm{diag}\left\{\mathrm{vec}\left\{\mathbf{\Omega}^{\mathrm{xb}}_k\right\}\right\}\\
&\quad\cdot\left(\mathbf{F}_{N_{\mathrm{c}}\times N_{\mathrm{g}}}\otimes\mathbf{V}_M\right)^H,\\
\mathbf{R}^{\mathrm{xv}}_{k,d} &\approx \beta^{\mathrm{xv}}_{k,d}\left(\mathbf{F}_{N_{\mathrm{c}}\times N_{\mathrm{g}}}\otimes\mathbf{V}_{N_d}\right)\mathrm{diag}\left\{\mathrm{vec}\left\{\mathbf{\Omega}^{\mathrm{xv}}_{k,d}\right\}\right\}\\
&\quad\cdot\left(\mathbf{F}_{N_{\mathrm{c}}\times N_{\mathrm{g}}}\otimes\mathbf{V}_{N_d}\right)^H,
\end{aligned} \tag{3}$$

for $\mathrm{x}\in\{\mathrm{c},\mathrm{v}\}$, where β^{xb}_k and $\beta^{\mathrm{xv}}_{k,d}$ are the large-scale fading coefficients of the channels in corresponding links, $\mathbf{V}_M$ and $\mathbf{V}_{N_d}$ are both unitary matrices depending on the antenna array topology equipped at the BS and VRx, respectively, and elements of $\mathrm{vec}\left\{\mathbf{\Omega}^{\mathrm{xb}}_k\right\}$ and $\mathrm{vec}\left\{\mathbf{\Omega}^{\mathrm{xv}}_{k,d}\right\}$, which depend on the corresponding channel power spectra in the AD domain, are the eigenvalues of $\mathbf{R}^{\mathrm{xb}}_k$ and $\mathbf{R}^{\mathrm{xv}}_{k,d}$, respectively.

Considering that it is rather difficult to obtain the large dimensional $\mathbf{R}^{\mathrm{xb}}_k$ and $\mathbf{R}^{\mathrm{xv}}_{k,d}$ in practice, motivated by (3), we have the following decompositions

$$\begin{aligned}
\mathbf{G}^{\mathrm{xb}}_{k,\ell} &= \mathbf{V}_M\mathbf{H}^{\mathrm{xb}}_{k,\ell}\mathbf{F}^T_{N_{\mathrm{c}}\times N_{\mathrm{g}}},\\
\mathbf{G}^{\mathrm{xv}}_{k,d,\ell} &= \mathbf{V}_{N_d}\mathbf{H}^{\mathrm{xv}}_{k,d,\ell}\mathbf{F}^T_{N_{\mathrm{c}}\times N_{\mathrm{g}}},
\end{aligned} \tag{4}$$

where $\mathbf{H}^{\mathrm{xb}}_{k,\ell} \in \mathbb{C}^{M\times N_{\mathrm{g}}}$ and $\mathbf{H}^{\mathrm{xv}}_{k,d,\ell} \in \mathbb{C}^{N_d\times N_{\mathrm{g}}}$ are the corresponding AD domain channel response matrices (ADCRMs) at the ℓth OFDM symbol. Then when $M, N_d \to \infty$, we have the following statistical property [8]

$$\begin{aligned}
&\mathrm{E}\left\{\left[\mathbf{H}^{\mathrm{xb}}_{k,\ell+\Delta_\ell}\right]_{i,j}\left[\mathbf{H}^{\mathrm{xb}}_{k,\ell}\right]^*_{i',j'}\right\}\\
&\quad=\beta^{\mathrm{xb}}_k\tau^{\mathrm{xb}}_k(\Delta_\ell)\,\delta(i-i')\,\delta(j-j')\cdot\left[\mathbf{\Omega}^{\mathrm{xb}}_k\right]_{i,j},\\
&\mathrm{E}\left\{\left[\mathbf{H}^{\mathrm{xv}}_{k,d,\ell+\Delta_\ell}\right]_{i,j}\left[\mathbf{H}^{\mathrm{xv}}_{k,d,\ell}\right]^*_{i',j'}\right\}\\
&\quad=\beta^{\mathrm{xv}}_{k,d}\tau^{\mathrm{xv}}_{k,d}(\Delta_\ell)\,\delta(i-i')\,\delta(j-j')\cdot\left[\mathbf{\Omega}^{\mathrm{xv}}_{k,d}\right]_{i,j}.
\end{aligned}\tag{5}$$

Note that $\left[\mathbf{\Omega}^{\mathrm{xb}}_k\right]_{i,j}$ and $\left[\mathbf{\Omega}^{\mathrm{xv}}_{k,d}\right]_{i,j}$ correspond to the average power of $\left[\mathbf{H}^{\mathrm{xb}}_k\right]_{i,j}$ and $\left[\mathbf{H}^{\mathrm{xv}}_{k,d}\right]_{i,j}$, respectively, and can represent the sparsity of the wireless channels in the AD domain. Hereafter we will refer to $\mathbf{\Omega}^{\mathrm{xb}}_k$ and $\mathbf{\Omega}^{\mathrm{xv}}_{k,d}$ as the corresponding AD domain channel power matrices (ADCPMs). (5) indicates the statistical uncorrelation for different elements of the ADCRMs and thus the ADCPMs $\mathbf{\Omega}^{\mathrm{xb}}_k$ and $\mathbf{\Omega}^{\mathrm{xv}}_{k,d}$, the dimensions of which are much smaller than those of $\mathbf{R}^{\mathrm{xb}}_k$ and $\mathbf{R}^{\mathrm{xv}}_{k,d}$, can be estimated element-by-element. We assume that all the ADCPMs are known at the BS and all the VRxs.

To simplify the following analyses, we extend $\mathbf{G}^{\mathrm{xb}}_{k,\ell}$ and $\mathbf{H}^{\mathrm{xv}}_{k,d,\ell}$ as follows

$$\begin{aligned}
\bar{\mathbf{H}}^{\mathrm{xb}}_{k,\ell,(N_{\mathrm{c}})} &\triangleq \mathbf{H}^{\mathrm{xb}}_{k,\ell}\mathbf{I}^T_{N_{\mathrm{c}}\times N_{\mathrm{g}}}\\
&=\left[\mathbf{H}^{\mathrm{xb}}_{k,\ell}\quad\mathbf{0}_{M\times(N_{\mathrm{c}}-N_{\mathrm{g}})}\right]\in\mathbb{C}^{M\times N_{\mathrm{c}}},\\
\bar{\mathbf{H}}^{\mathrm{xv}}_{k,d,\ell,(N_{\mathrm{c}})} &\triangleq \mathbf{H}^{\mathrm{xv}}_{k,d,\ell}\mathbf{I}^T_{N_{\mathrm{c}}\times N_{\mathrm{g}}}\\
&=\left[\mathbf{H}^{\mathrm{xv}}_{k,d,\ell}\quad\mathbf{0}_{N_d\times(N_{\mathrm{c}}-N_{\mathrm{g}})}\right]\in\mathbb{C}^{N_d\times N_{\mathrm{c}}},
\end{aligned}\tag{6}$$

for $\mathrm{x}\in\{\mathrm{c},\mathrm{v}\}$. Similarly, the corresponding extended ADCPMs are defined as

$$\begin{aligned}
\bar{\mathbf{\Omega}}^{\mathrm{xb}}_{k,(N_{\mathrm{c}})} &\triangleq \mathbf{\Omega}^{\mathrm{xb}}_k\mathbf{I}^T_{N_{\mathrm{c}}\times N_{\mathrm{g}}}\\
&=\left[\mathbf{\Omega}^{\mathrm{xb}}_k\quad\mathbf{0}_{M\times(N_{\mathrm{c}}-N_{\mathrm{g}})}\right]\in\mathbb{R}^{M\times N_{\mathrm{c}}},\\
\bar{\mathbf{\Omega}}^{\mathrm{xv}}_{k,d,(N_{\mathrm{c}})} &\triangleq \mathbf{\Omega}^{\mathrm{xv}}_{k,d}\mathbf{I}^T_{N_{\mathrm{c}}\times N_{\mathrm{g}}}\\
&=\left[\mathbf{\Omega}^{\mathrm{xv}}_{k,d}\quad\mathbf{0}_{N_d\times(N_{\mathrm{c}}-N_{\mathrm{g}})}\right]\in\mathbb{R}^{N_d\times N_{\mathrm{c}}},
\end{aligned}\tag{7}$$

respectively.

III. CHANNEL ESTIMATION WITH PSAPs

We propose PSAPs for V2V underlay mMIMO-OFDM and investigate the CE performance with PSAPs in this section.

Assume that pilot signals are simultaneously sent from all the CUs and VTxs over the ℓth OFDM symbol, then the received signals at the BS and the dth VRx in the SF domain can be represented by

$$\begin{aligned}
\mathbf{Y}^{\mathrm{b}}_{\ell} &= \sum_{k'=0}^{K-1}\mathbf{G}^{\mathrm{cb}}_{k',\ell}\mathbf{X}_{k'}+\sum_{i'=0}^{D-1}\mathbf{G}^{\mathrm{vb}}_{i',\ell}\mathbf{X}_{i'}+\mathbf{Z}^{\mathrm{b}}_{\ell}\in\mathbb{C}^{M\times N_{\mathrm{c}}},\\
\mathbf{Y}^{\mathrm{v}}_{d,\ell} &= \sum_{k'=0}^{K-1}\mathbf{G}^{\mathrm{cv}}_{k',d,\ell}\mathbf{X}_{k'}+\sum_{i'=0}^{D-1}\mathbf{G}^{\mathrm{vv}}_{i',d,\ell}\mathbf{X}_{i'}+\mathbf{Z}^{\mathrm{v}}_{d,\ell}\in\mathbb{C}^{N_d\times N_{\mathrm{c}}},
\end{aligned}\tag{8}$$

where $\mathbf{X}_{k'}=\mathrm{diag}\{\mathbf{x}_{k'}\}\in\mathbb{C}^{N_{\mathrm{c}}\times N_{\mathrm{c}}}$ and $\mathbf{X}_{i'}=\mathrm{diag}\{\mathbf{x}_{i'}\}\in\mathbb{C}^{N_{\mathrm{c}}\times N_{\mathrm{c}}}$ denote the pilots in the frequency domain transmitted from the k'th CU and the i'th VTx, respectively, $\mathbf{Z}^{\mathrm{b}}_{\ell}$ and $\mathbf{Z}^{\mathrm{v}}_{d,\ell}$

$$\begin{aligned}
\mathbf{Y}^{\mathrm{b}}_{k,\ell} &= \frac{1}{\sigma_{\mathrm{t}}}\mathbf{V}^H_M\mathbf{Y}^{\mathrm{b}}_{\ell}\mathbf{X}^H_k\mathbf{F}^*_{N_{\mathrm{c}}\times N_{\mathrm{g}}}\\
&\overset{(a)}{=}\mathbf{H}^{\mathrm{cb}}_{k,\ell}+\underbrace{\sum_{k'\neq k}\mathbf{H}^{\mathrm{cb}}_{k',\ell}\mathbf{F}^T_{N_{\mathrm{c}}\times N_{\mathrm{g}}}\mathbf{D}_{\phi_{k'}-\phi_k}\mathbf{F}^*_{N_{\mathrm{c}}\times N_{\mathrm{g}}}}_{\text{PI from CUs}\triangleq\sum_{k'\neq k}\mathbf{H}^{\mathrm{cb},\phi_{k'}-\phi_k}_{k',\ell}}+\underbrace{\sum_{d'=0}^{D-1}\mathbf{H}^{\mathrm{vb}}_{d',\ell}\mathbf{F}^T_{N_{\mathrm{c}}\times N_{\mathrm{g}}}\mathbf{D}_{\phi_{d'}-\phi_k}\mathbf{F}^*_{N_{\mathrm{c}}\times N_{\mathrm{g}}}}_{\text{PI from VTxs}\triangleq\sum_{d'=0}^{D-1}\mathbf{H}^{\mathrm{vb},\phi_{d'}-\phi_k}_{d',\ell}}+\underbrace{\frac{1}{\sigma_{\mathrm{t}}}\mathbf{V}^H_M\mathbf{Z}^{\mathrm{b}}_{\ell}\mathbf{X}^H_k\mathbf{F}^*_{N_{\mathrm{c}}\times N_{\mathrm{g}}}}_{\text{noise}}\\
&\overset{(b)}{=}\mathbf{H}^{\mathrm{cb}}_{k,\ell}+\sum_{k'\neq k}\mathbf{H}^{\mathrm{cb},\phi_{k'}-\phi_k}_{k',\ell}+\sum_{d'=0}^{D-1}\mathbf{H}^{\mathrm{vb},\phi_{d'}-\phi_k}_{d',\ell}+\frac{\sqrt{\sigma_{\mathrm{z}}}}{\sqrt{\sigma_{\mathrm{t}}}}\mathbf{Z}^{\mathrm{iid}}_k
\end{aligned}\tag{11}$$

$$\begin{aligned}
\mathbf{Y}^{\mathrm{v}}_{d,d,\ell} &= \frac{1}{\sigma_{\mathrm{t}}}\mathbf{V}^H_{N_d}\mathbf{Y}^{\mathrm{v}}_{d,\ell}\mathbf{X}^H_d\mathbf{F}^*_{N_{\mathrm{c}}\times N_{\mathrm{g}}}\\
&=\mathbf{H}^{\mathrm{vb}}_{d,d,\ell}+\underbrace{\sum_{d'\neq d}\mathbf{H}^{\mathrm{vv}}_{d',d,\ell}\mathbf{F}^T_{N_{\mathrm{c}}\times N_{\mathrm{g}}}\mathbf{D}_{\phi_{d'}-\phi_d}\mathbf{F}^*_{N_{\mathrm{c}}\times N_{\mathrm{g}}}}_{\text{PI from VTxs}\triangleq\sum_{d'\neq d}\mathbf{H}^{\mathrm{vv},\phi_{d'}-\phi_d}_{d',d,\ell}}+\underbrace{\sum_{k'=0}^{K-1}\mathbf{H}^{\mathrm{cv}}_{k',d,\ell}\mathbf{F}^T_{N_{\mathrm{c}}\times N_{\mathrm{g}}}\mathbf{D}_{\phi_{k'}-\phi_d}\mathbf{F}^*_{N_{\mathrm{c}}\times N_{\mathrm{g}}}}_{\text{PI from CUs}\triangleq\sum_{k'=0}^{K-1}\mathbf{H}^{\mathrm{cv},\phi_{k'}-\phi_d}_{k',d,\ell}}+\underbrace{\frac{1}{\sigma_{\mathrm{t}}}\mathbf{V}^H_{N_d}\mathbf{Z}^{\mathrm{v}}_{d,\ell}\mathbf{X}^H_d\mathbf{F}^*_{N_{\mathrm{c}}\times N_{\mathrm{g}}}}_{\text{noise}}\\
&=\mathbf{H}^{\mathrm{vb}}_{d,d,\ell}+\sum_{d'\neq d}\mathbf{H}^{\mathrm{vv},\phi_{d'}-\phi_d}_{d',d,\ell}+\sum_{k'=0}^{K-1}\mathbf{H}^{\mathrm{cv},\phi_{k'}-\phi_d}_{k',d,\ell}+\frac{\sqrt{\sigma_{\mathrm{z}}}}{\sqrt{\sigma_{\mathrm{t}}}}\mathbf{Z}^{\mathrm{iid}}_{d,d}
\end{aligned}\tag{12}$$

are the additive white Gaussian noise (AWGN) matrices with elements identically and independently distributed (i.i.d.) as $\mathcal{CN}(0, \sigma_z)$, and σ_z denotes the noise power.

The proposed PSAP for a given CU or VTx i is shown by

$$\mathbf{X}_i \triangleq \sqrt{\sigma_t}\mathrm{diag}\left\{\mathbf{f}_{N_c,\phi_i}\right\}\mathbf{X}, \quad \phi_i = 0, 1, \ldots, N_c - 1, \quad (9)$$

where $\mathbf{X}$ is an arbitrary diagonal matrix satisfying $\mathbf{X}\mathbf{X}^H = \mathbf{I}_{N_c}$, and σ_t denotes the pilot signal transmit power. Define $\mathbf{D}_{\phi_k} \triangleq \mathrm{diag}\left\{\mathbf{f}_{N_c,\phi_k}\right\}$, and we can obtain from (9) that, for $\forall i, i' \in \mathcal{K} \cup \mathcal{V}_{\mathrm{Tx}}$,

$$\mathbf{X}_{i'}\mathbf{X}_i^H = \sigma_t \mathbf{D}_{\phi_{i'}-\phi_i}, \quad (10)$$

which indicates that only the phase shift differences between different users have influence on the corresponding cross correlations of the proposed PSAPs.

After decorrelating the received signals, the power normalized observation obtained at the BS for the channel $\mathbf{H}_{k,\ell}^{\mathrm{cb}}$ of the kth CU is given by (11), as shown at the bottom of the previous page, where (a) derives from (4) and (10), (b) derives from the unitary transformation property, elements in the normalized AWGN matrix $\mathbf{Z}_k^{\mathrm{iid}} \in \mathbb{C}^{M\times N_g}$ are distributed as $\mathcal{CN}(0, 1)$, and the term PI means pilot interference. Similarly, the dth VRx can obtain the corresponding observation for the dth VTx shown by (12), as shown at the bottom of the previous page.

The PI from CUs defined in (11) satisfies

$$\begin{aligned}\mathbf{H}_{k',\ell}^{\mathrm{cb},\phi_{k'}-\phi_k} &=^{(a)} \bar{\mathbf{H}}_{k',\ell,(N_c)}^{\mathrm{cb}}\mathbf{F}_{N_c}^T\mathbf{D}_{\phi_{k'}-\phi_k}\mathbf{F}_{N_c}^*\mathbf{I}_{N_c\times N_g}\\ &=^{(b)} \bar{\mathbf{H}}_{k',\ell,(N_c)}^{\mathrm{cb}}\mathbf{\Pi}_{N_c}^{\phi_{k'}-\phi_k}\mathbf{I}_{N_c\times N_g}, \end{aligned} \quad (13)$$

where (a) derives from (6), and (b) derives from the definition of the permutation matrix $\mathbf{\Pi}_N^n$. From (13), we can see that $\mathbf{H}_{k',\ell}^{\mathrm{cb},\phi_{k'}-\phi_k}$ can be obtained by implementing $\phi_{k'} - \phi_k$ cyclic column shift and then the first N_g column truncation to the extended ADCRM $\bar{\mathbf{H}}_{k',\ell}^{\mathrm{cb}}$. Recalling (5), it is readily shown that elements of $\mathbf{H}_{k',\ell}^{\mathrm{cb},\phi_{k'}-\phi_k}$ are statistically uncorrelated. Thus, we have the following definition

$$\begin{aligned}\mathbf{\Omega}_{k'}^{\mathrm{cb},\phi_{k'}-\phi_k} &\triangleq \mathrm{E}\left\{\mathbf{H}_{k',\ell}^{\mathrm{cb},\phi_{k'}-\phi_k} \odot \left(\mathbf{H}_{k',\ell}^{\mathrm{cb},\phi_{k'}-\phi_k}\right)^*\right\}\\ &= \bar{\mathbf{\Omega}}_{k',(N_c)}^{\mathrm{cb}}\mathbf{\Pi}_{N_c}^{\phi_{k'}-\phi_k}\mathbf{I}_{N_c\times N_g}, \end{aligned} \quad (14)$$

which represents the corresponding power matrix of $\mathbf{H}_{k',\ell}^{\mathrm{cb},\phi_{k'}-\phi_k}$ and can be obtained by implementing the same cyclic column shift and column truncation to the extended ADCPM $\bar{\mathbf{\Omega}}_{k',(N_c)}^{\mathrm{cb}}$ defined in (7). Meanwhile, $\mathbf{H}_{d',\ell}^{\mathrm{vb},\phi_{d'}-\phi_k}$,$\mathbf{H}_{d',d,\ell}^{\mathrm{vv},\phi_{d'}-\phi_d}$, $\mathbf{H}_{k',d,\ell}^{\mathrm{cv},\phi_{k'}-\phi_d}$ defined in (11) and (12) and their corresponding power matrices satisfy similar expressions as in (13) and (14).

From (5), it can be known that elements of the AD domain channel are uncorrelated. Thus we can obtain the MMSE estimates at the BS for CU k and at the dth VRx for VTx d in an element-wise manner, which are given by (15), as shown at the bottom of the page, and the corresponding MSEs are shown in (16) and (17), as shown at the bottom of the page.

Define the sMSE of all the CUs at the BS and the sMSE of all the VTxs at the corresponding VRxs for CE as

$$\begin{aligned}\epsilon^{\mathrm{b,CE}} &\triangleq \sum_{k=0}^{K-1}\epsilon_k^{\mathrm{cb,CE}},\\ \epsilon^{\mathrm{v,CE}} &\triangleq \sum_{d=0}^{D-1}\epsilon_d^{\mathrm{vv,CE}}. \end{aligned} \quad (18)$$

$$\begin{aligned}\left[\hat{\mathbf{H}}_{k,\ell}^{\mathrm{cb}}\right]_{i,j} &= \frac{\beta_k^{\mathrm{cb}}\left[\mathbf{\Omega}_k^{\mathrm{cb}}\right]_{i,j}}{\sum_{k'=0}^{K-1}\beta_{k'}^{\mathrm{cb}}\left[\mathbf{\Omega}_{k'}^{\mathrm{cb},\phi_{k'}-\phi_k}\right]_{i,j}+\sum_{d'=0}^{D-1}\beta_{d'}^{\mathrm{vb}}\left[\mathbf{\Omega}_{d'}^{\mathrm{vb},\phi_{d'}-\phi_k}\right]_{i,j}+\frac{\sigma_z}{\sigma_t}}\left[\mathbf{Y}_{k,\ell}^{\mathrm{b}}\right]_{i,j}\\ \left[\hat{\mathbf{H}}_{d,d,\ell}^{\mathrm{vv}}\right]_{i,j} &= \frac{\beta_{d,d}^{\mathrm{vv}}\left[\mathbf{\Omega}_{d,d}^{\mathrm{vv}}\right]_{i,j}}{\sum_{d'=0}^{D-1}\beta_{d',d}^{\mathrm{vv}}\left[\mathbf{\Omega}_{d',d}^{\mathrm{vv},\phi_{d'}-\phi_d}\right]_{i,j}+\sum_{k'=0}^{K-1}\beta_{k',d}^{\mathrm{cv}}\left[\mathbf{\Omega}_{k'}^{\mathrm{cv},\phi_{k'}-\phi_d}\right]_{i,j}+\frac{\sigma_z}{\sigma_t}}\left[\mathbf{Y}_{d,d,\ell}^{\mathrm{v}}\right]_{i,j} \end{aligned} \quad (15)$$

$$\begin{aligned}\epsilon_k^{\mathrm{cb,CE}} &\triangleq \sum_{i=0}^{M-1}\sum_{j=0}^{N_g-1}\mathrm{E}\left\{\left|\left[\mathbf{H}_{k,\ell}^{\mathrm{cb}}-\hat{\mathbf{H}}_{k,\ell}^{\mathrm{cb}}\right]_{i,j}\right|^2\right\}=\sum_{i=0}^{M-1}\sum_{j=0}^{N_g-1}\mathrm{E}\left\{\left|\left[\mathbf{H}_{k,\ell}^{\mathrm{cb}}\right]_{i,j}\right|^2-\left|\left[\hat{\mathbf{H}}_{k,\ell}^{\mathrm{cb}}\right]_{i,j}\right|^2\right\}\\ &=\sum_{i=0}^{M-1}\sum_{j=0}^{N_g-1}\left\{\beta_k^{\mathrm{cb}}\left[\mathbf{\Omega}_k^{\mathrm{cb}}\right]_{i,j}-\frac{(\beta_k^{\mathrm{cb}})^2\left[\mathbf{\Omega}_k^{\mathrm{cb}}\right]_{i,j}^2}{\sum_{k'=0}^{K-1}\beta_{k'}^{\mathrm{cb}}\left[\mathbf{\Omega}_{k'}^{\mathrm{cb},\phi_{k'}-\phi_k}\right]_{i,j}+\sum_{d'=0}^{D-1}\beta_{d'}^{\mathrm{vb}}\left[\mathbf{\Omega}_{d'}^{\mathrm{vb},\phi_{d'}-\phi_k}\right]_{i,j}+\frac{\sigma_z}{\sigma_t}}\right\} \end{aligned} \quad (16)$$

$$\epsilon_{d,d}^{\mathrm{vv,CE}}=\sum_{i=0}^{N_d-1}\sum_{j=0}^{N_g-1}\left\{\beta_{d,d}^{\mathrm{vv}}\left[\mathbf{\Omega}_{d,d}^{\mathrm{vv}}\right]_{i,j}-\frac{(\beta_{d,d}^{\mathrm{vv}})^2\left[\mathbf{\Omega}_{d,d}^{\mathrm{vv}}\right]_{i,j}^2}{\sum_{d'=0}^{D-1}\beta_{d',d}^{\mathrm{vv}}\left[\mathbf{\Omega}_{d',d}^{\mathrm{vv},\phi_{d'}-\phi_d}\right]_{i,j}+\sum_{k'=0}^{K-1}\beta_{k',d}^{\mathrm{cv}}\left[\mathbf{\Omega}_{k',d}^{\mathrm{cv},\phi_{k'}-\phi_d}\right]_{i,j}+\frac{\sigma_z}{\sigma_t}}\right\} \quad (17)$$

Then in the following proposition, we derive the optimal condition under which the sMSEs defined in (18) can both be minimized.

Proposition 1: The sMSE $\epsilon^{\mathrm{b,CE}}$ can be minimized as

$$\varepsilon^{\mathrm{b,CE}}=\sum_{k=0}^{K-1}\sum_{i=0}^{M-1}\sum_{j=0}^{N_{\mathrm{g}}-1}\left\{\beta_k^{\mathrm{cb}}\left[\mathbf{\Omega}_k^{\mathrm{cb}}\right]_{i,j}-\frac{(\beta_k^{\mathrm{cb}})^2\left[\mathbf{\Omega}_k^{\mathrm{cb}}\right]_{i,j}^2}{\beta_k^{\mathrm{cb}}\left[\mathbf{\Omega}_k^{\mathrm{cb}}\right]_{i,j}+\frac{\sigma_{\mathrm{z}}}{\sigma_{\mathrm{t}}}}\right\} \tag{19}$$

and the corresponding optimal condition is that for $\forall k\neq k'\in\mathcal{K}$ and $\forall d\in\mathcal{V}_{\mathrm{Tx}}$,

$$\begin{aligned}&\left(\bar{\mathbf{\Omega}}_{k,(N_{\mathrm{c}})}^{\mathrm{cb}}\mathbf{\Pi}_{N_{\mathrm{c}}}^{\phi_k}\right)\odot\left(\bar{\mathbf{\Omega}}_{k',(N_{\mathrm{c}})}^{\mathrm{cb}}\mathbf{\Pi}_{N_{\mathrm{c}}}^{\phi_{k'}}\right)\\&\quad=\left(\bar{\mathbf{\Omega}}_{k,(N_{\mathrm{c}})}^{\mathrm{cb}}\mathbf{\Pi}_{N_{\mathrm{c}}}^{\phi_k}\right)\odot\left(\bar{\mathbf{\Omega}}_{d,(N_{\mathrm{c}})}^{\mathrm{vb}}\mathbf{\Pi}_{N_{\mathrm{c}}}^{\phi_d}\right)=\mathbf{0}.\end{aligned} \tag{20}$$

In addition, the sMSE $\epsilon^{\mathrm{v,CE}}$ can be minimized as

$$\varepsilon^{\mathrm{v,CE}}=\sum_{d=0}^{D-1}\sum_{i=0}^{N_d-1}\sum_{j=0}^{N_{\mathrm{g}}-1}\left\{\beta_{d,d}^{\mathrm{vv}}\left[\mathbf{\Omega}_{d,d}^{\mathrm{vv}}\right]_{i,j}-\frac{(\beta_{d,d}^{\mathrm{vv}})^2\left[\mathbf{\Omega}_{d,d}^{\mathrm{vv}}\right]_{i,j}^2}{\beta_{d,d}^{\mathrm{vv}}\left[\mathbf{\Omega}_{d,d}^{\mathrm{vv}}\right]_{i,j}+\frac{\sigma_{\mathrm{z}}}{\sigma_{\mathrm{t}}}}\right\} \tag{21}$$

and the corresponding optimal condition is that for $\forall d\neq d'\in\mathcal{V}_{\mathrm{Tx}}$ and $\forall k\in\mathcal{K}$,

$$\begin{aligned}&\left(\bar{\mathbf{\Omega}}_{d,d,(N_{\mathrm{c}})}^{\mathrm{vv}}\mathbf{\Pi}_{N_{\mathrm{c}}}^{\phi_d}\right)\odot\left(\bar{\mathbf{\Omega}}_{d',d,(N_{\mathrm{c}})}^{\mathrm{vv}}\mathbf{\Pi}_{N_{\mathrm{c}}}^{\phi_{d'}}\right)\\&\quad=\left(\bar{\mathbf{\Omega}}_{d,d,(N_{\mathrm{c}})}^{\mathrm{vv}}\mathbf{\Pi}_{N_{\mathrm{c}}}^{\phi_d}\right)\odot\left(\bar{\mathbf{\Omega}}_{k,d,(N_{\mathrm{c}})}^{\mathrm{cv}}\mathbf{\Pi}_{N_{\mathrm{c}}}^{\phi_k}\right)=\mathbf{0}.\end{aligned} \tag{22}$$

Proof: See Appendix A. ∎

The physical explanation of Propsition 1 is that the PI among users can be eliminated when the non-overlapping property for the equivalent AD domain channel power spectra of different CUs and VTxs are satisfied after proper pilot phase shift allocation, and thus the optimal sMSE performance can be achieved. Note that wireless channels in many practical propagation scenarios satisfy the sparse property in the AD domain [13]–[15], which suggests that the proposed approach is feasible for V2V underlay mMIMO-OFDM. Thus, in our proposed approach, the phase shifts for different pilots are adjustable and pilots with the same pilot shift can even be allocated to different users, leading to more available pilots.

IV. CHANNEL PREDICTION WITH PSAPS

Taking into account the high mobility scenario and the fast V2V channel fading, it might be improper to directly utilize the channel estimates of the pilot segment for the transmission during the data segment. In this section, CP based on the PSAPs is investigated for the data segment in V2V underlay mMIMO-OFDM.

With the statistical property of the ADCRM given in (5), we can see that an estimate of $\mathbf{H}_{k,\ell+\Delta_\ell}^{\mathrm{cb}}$ at the BS for CU k and an estimate of $\mathbf{H}_{d,d,\ell+\Delta_\ell}^{\mathrm{vv}}$ at VRx d for VTx d can be obtained element-by-element under the MMSE criterion, as given in (23), as shown at the bottom of the next page. From (23) and (15), it can be easily obtained that

$$\begin{aligned}\hat{\mathbf{H}}_{k,\ell+\Delta_\ell}^{\mathrm{cb}}&=\tau_k^{\mathrm{cb}}(\Delta_\ell)\,\hat{\mathbf{H}}_{k,\ell}^{\mathrm{cb}},\\\hat{\mathbf{H}}_{d,d,\ell+\Delta_\ell}^{\mathrm{vv}}&=\tau_{d,d}^{\mathrm{vv}}(\Delta_\ell)\,\hat{\mathbf{H}}_{d,d,\ell}^{\mathrm{vv}}.\end{aligned} \tag{24}$$

From (24), we can immediately obtain the channel estimates in the data segment via the corresponding channel TCFs and the channel estimates of the pilot segment, which reduces the complexity of CP.

Similar to (18), the sMSE of CP for a given delay Δ_ℓ is defined as in (25), as shown at the bottom of the next page. In the following proposition, we will show that the PI affects among users can still be eliminated with the pilot phase shifts properly allocated.

Proposition 2: The sMSE $\epsilon^{\mathrm{b,CP}}(\Delta_\ell)\ \forall\Delta_\ell$ can be minimized as

$$\begin{aligned}\varepsilon^{\mathrm{b,CP}}(\Delta_\ell)=&\sum_{k=0}^{K-1}\sum_{i=0}^{M-1}\sum_{j=0}^{N_{\mathrm{g}}-1}\\&\left\{\beta_k^{\mathrm{cb}}\left[\mathbf{\Omega}_k^{\mathrm{cb}}\right]_{i,j}-\left[\beta_k^{\mathrm{cb}}\tau_k^{\mathrm{cb}}(\Delta_\ell)\right]^2\frac{\left[\mathbf{\Omega}_k^{\mathrm{cb}}\right]_{i,j}^2}{\beta_k^{\mathrm{cb}}\left[\mathbf{\Omega}_k^{\mathrm{cb}}\right]_{i,j}+\frac{\sigma_{\mathrm{ztr}}}{\sigma_{\mathrm{xtr}}}}\right\}\end{aligned} \tag{26}$$

and the corresponding optimal condition is that for $\forall k\neq k'\in\mathcal{K}$ and $\forall d\in\mathcal{V}_{\mathrm{Tx}}$,

$$\begin{aligned}&\left(\bar{\mathbf{\Omega}}_{k,(N_{\mathrm{c}})}^{\mathrm{cb}}\mathbf{\Pi}_{N_{\mathrm{c}}}^{\phi_k}\right)\odot\left(\bar{\mathbf{\Omega}}_{k',(N_{\mathrm{c}})}^{\mathrm{cb}}\mathbf{\Pi}_{N_{\mathrm{c}}}^{\phi_{k'}}\right)\\&\quad=\left(\bar{\mathbf{\Omega}}_{k,(N_{\mathrm{c}})}^{\mathrm{cb}}\mathbf{\Pi}_{N_{\mathrm{c}}}^{\phi_k}\right)\odot\left(\bar{\mathbf{\Omega}}_{d,(N_{\mathrm{c}})}^{\mathrm{vb}}\mathbf{\Pi}_{N_{\mathrm{c}}}^{\phi_{d'}}\right)=\mathbf{0}.\end{aligned} \tag{27}$$

In addition, the sMSE $\epsilon^{\mathrm{v,CP}}(\Delta_\ell)\ \forall\Delta_\ell$ can be minimized as

$$\begin{aligned}\varepsilon^{\mathrm{v,CP}}(\Delta_\ell)=&\sum_{d=0}^{D-1}\sum_{i=0}^{N_d-1}\sum_{j=0}^{N_{\mathrm{g}}-1}\\&\left\{\beta_{d,d}^{\mathrm{vv}}\left[\mathbf{\Omega}_{d,d}^{\mathrm{vv}}\right]_{i,j}-\left[\beta_{d,d}^{\mathrm{vv}}\tau_{d,d}^{\mathrm{vv}}(\Delta_\ell)\right]^2\frac{\left[\mathbf{\Omega}_{d,d}^{\mathrm{vv}}\right]_{i,j}^2}{\beta_{d,d}^{\mathrm{vv}}\left[\mathbf{\Omega}_{d,d}^{\mathrm{vv}}\right]_{i,j}+\frac{\sigma_{\mathrm{ztr}}}{\sigma_{\mathrm{xtr}}}}\right\}\end{aligned} \tag{28}$$

and the corresponding optimal condition is that for $\forall d\neq d'\in\mathcal{V}_{\mathrm{Tx}}$ and $\forall k\in\mathcal{K}$,

$$\begin{aligned}&\left(\bar{\mathbf{\Omega}}_{d,d,(N_{\mathrm{c}})}^{\mathrm{vv}}\mathbf{\Pi}_{N_{\mathrm{c}}}^{\phi_d}\right)\odot\left(\bar{\mathbf{\Omega}}_{d',d,(N_{\mathrm{c}})}^{\mathrm{vv}}\mathbf{\Pi}_{N_{\mathrm{c}}}^{\phi_{d'}}\right)\\&\quad=\left(\bar{\mathbf{\Omega}}_{d,d,(N_{\mathrm{c}})}^{\mathrm{vv}}\mathbf{\Pi}_{N_{\mathrm{c}}}^{\phi_d}\right)\odot\left(\bar{\mathbf{\Omega}}_{k,d,(N_{\mathrm{c}})}^{\mathrm{cv}}\mathbf{\Pi}_{N_{\mathrm{c}}}^{\phi_k}\right)=\mathbf{0}.\end{aligned} \tag{29}$$

Proof: The proof is similar to that of Propsition 1, and is omitted for brevity. ∎

Propsition 2 shows that the optimal pilot phase shift allocation condition for CE is still applicable to CP, which indicates that the optimal performance of CE and CP can be achieved simultaneously with proper pilot allocation.

V. PILOT PHASE SHIFT ALLOCATION

Note that the optimal condition (20) and (22) cannot always be satisfied in practice, especially at the same time, which means the importance of proper pilot allocation. Considering the high computational complexity of the exhaustive search, we develop an ADCPS-PA algorithm combining the two optimal conditions in this section.

We first define some functions which represent the PI degree between two arbitrary transmitters in $\mathcal{K} \cup \mathcal{V}_{\mathrm{Tx}}$ for channel acquisition at the BS or some VRx as follows

$$\zeta^{\mathrm{b}}_{k,k'} \triangleq \frac{\beta^{\mathrm{cb}}_k \beta^{\mathrm{cb}}_{k'} \sum_{i,j}\left[\left(\bar{\mathbf{\Omega}}^{\mathrm{cb}}_{k,(N_{\mathrm{c}})}\mathbf{\Pi}^{\phi_k}_{N_{\mathrm{c}}}\right)\odot\left(\bar{\mathbf{\Omega}}^{\mathrm{cb}}_{k',(N_{\mathrm{c}})}\mathbf{\Pi}^{\phi_{k'}}_{N_{\mathrm{c}}}\right)\right]_{i,j}}{\sqrt{\sum_{i,j}\left[\bar{\mathbf{\Omega}}^{\mathrm{cb}}_{k,(N_{\mathrm{c}})}\mathbf{\Pi}^{\phi_k}_{N_{\mathrm{c}}}\right]^2_{i,j}}\cdot\sqrt{\sum_{i,j}\left[\bar{\mathbf{\Omega}}^{\mathrm{cb}}_{k',(N_{\mathrm{c}})}\mathbf{\Pi}^{\phi_{k'}}_{N_{\mathrm{c}}}\right]^2_{i,j}}},$$

$$\zeta^{\mathrm{b}}_{k,d} \triangleq \frac{\beta^{\mathrm{cb}}_k \beta^{\mathrm{vb}}_d \sum_{i,j}\left[\left(\bar{\mathbf{\Omega}}^{\mathrm{cb}}_{k,(N_{\mathrm{c}})}\mathbf{\Pi}^{\phi_k}_{N_{\mathrm{c}}}\right)\odot\left(\bar{\mathbf{\Omega}}^{\mathrm{vb}}_{d,(N_{\mathrm{c}})}\mathbf{\Pi}^{\phi_d}_{N_{\mathrm{c}}}\right)\right]_{i,j}}{\sqrt{\sum_{i,j}\left[\bar{\mathbf{\Omega}}^{\mathrm{cb}}_{k,(N_{\mathrm{c}})}\mathbf{\Pi}^{\phi_k}_{N_{\mathrm{c}}}\right]^2_{i,j}}\cdot\sqrt{\sum_{i,j}\left[\bar{\mathbf{\Omega}}^{\mathrm{vb}}_{d,(N_{\mathrm{c}})}\mathbf{\Pi}^{\phi_d}_{N_{\mathrm{c}}}\right]^2_{i,j}}},$$

$$\zeta^{\mathrm{v}}_{k,d,m} \triangleq \frac{\beta^{\mathrm{cv}}_{k,m}\beta^{\mathrm{vv}}_{d,m} \sum_{i,j}\left[\left(\bar{\mathbf{\Omega}}^{\mathrm{cv}}_{k,m,(N_{\mathrm{c}})}\mathbf{\Pi}^{\phi_k}_{N_{\mathrm{c}}}\right)\odot\left(\bar{\mathbf{\Omega}}^{\mathrm{vv}}_{d,m,(N_{\mathrm{c}})}\mathbf{\Pi}^{\phi_d}_{N_{\mathrm{c}}}\right)\right]_{i,j}}{\sqrt{\sum_{i,j}\left[\bar{\mathbf{\Omega}}^{\mathrm{cv}}_{k,m,(N_{\mathrm{c}})}\mathbf{\Pi}^{\phi_k}_{N_{\mathrm{c}}}\right]^2_{i,j}}\cdot\sqrt{\sum_{i,j}\left[\bar{\mathbf{\Omega}}^{\mathrm{vv}}_{d,m,(N_{\mathrm{c}})}\mathbf{\Pi}^{\phi_d}_{N_{\mathrm{c}}}\right]^2_{i,j}}},$$

$$\zeta^{\mathrm{v}}_{d,d',m} \triangleq \frac{\beta^{\mathrm{vv}}_{d,m}\beta^{\mathrm{vv}}_{d',m} \sum_{i,j}\left[\left(\bar{\mathbf{\Omega}}^{\mathrm{vv}}_{d,m,(N_{\mathrm{c}})}\mathbf{\Pi}^{\phi_d}_{N_{\mathrm{c}}}\right)\odot\left(\bar{\mathbf{\Omega}}^{\mathrm{vv}}_{d',m,(N_{\mathrm{c}})}\mathbf{\Pi}^{\phi_{d'}}_{N_{\mathrm{c}}}\right)\right]_{i,j}}{\sqrt{\sum_{i,j}\left[\bar{\mathbf{\Omega}}^{\mathrm{vv}}_{d,m,(N_{\mathrm{c}})}\mathbf{\Pi}^{\phi_d}_{N_{\mathrm{c}}}\right]^2_{i,j}}\cdot\sqrt{\sum_{i,j}\left[\bar{\mathbf{\Omega}}^{\mathrm{vv}}_{d',m,(N_{\mathrm{c}})}\mathbf{\Pi}^{\phi_{d'}}_{N_{\mathrm{c}}}\right]^2_{i,j}}}, \tag{30}$$

where $k, k' \in \mathcal{K}$, $d, d' \in \mathcal{V}_{\mathrm{Tx}}$, $m \in \mathcal{V}_{\mathrm{Rx}}$. Then we define a degree of relevance between two given transmitter sets $\mathcal{A}$ and $\mathcal{B}$ as

$$\mathrm{DR}(\mathcal{A},\mathcal{B}) \triangleq \sum_{\substack{k,d\in\mathcal{A},\\ k',d'\in\mathcal{B}}} \zeta^{\mathrm{b}}_{k,k'}+\zeta^{\mathrm{b}}_{k,d'}+\zeta^{\mathrm{b}}_{d,k'}+\zeta^{\mathrm{v}}_{k,d',d'}+\zeta^{\mathrm{v}}_{d,d',d'}+\zeta^{\mathrm{v}}_{d,d',d}, \tag{31}$$

where both $\mathcal{A}$ and $\mathcal{B}$ can contain CUs and VTxs. It is obvious that for transmitters in $\mathcal{A}$ and $\mathcal{B}$, the value of $\mathrm{DR}(\mathcal{A},\mathcal{B})$ depends on the overlapping degree of their equivalent AD domain channel power spectra and lower overlapping degree leads to smaller $\mathrm{DR}(\mathcal{A},\mathcal{B})$. When their equivalent channel power distributions are non-overlapping, $\mathrm{DR}(\mathcal{A},\mathcal{B}) = 0$ and the PI between the two transmitter sets is eliminated.

With the definitions presented above, the ADCPS-PA algorithm is displayed in Algorithm 1. The output of Algorithm 1 is the pilot phase shift pattern, which is defined as $\{\phi_i : i \in \mathcal{T}, \mathcal{T} = \mathcal{K} \cup \mathcal{V}_{\mathrm{Tx}}\}$. The threshold γ is preset to balance the algorithm complexity and the performance of channel acquisition, where smaller γ leads to better channel acquisition performance but higher algorithm complexity. $\mathcal{T}^{\mathrm{sch}}$ denotes the user set in which users have been allocated pilot phase shifts after proper scheduling, and $\mathcal{T}^{\mathrm{un}}$ denotes the user set in which users have not been allocated pilot phase shifts.

VI. SIMULATION RESULTS

In this section, we show the simulation results and analyze the channel acquisition performance with the proposed PSAPs in V2V underlay mMIMO-OFDM transmission. Note that the approximations in (3) are tight enough with a relatively large and practically feasible number of antennas (64 to 512),

$$\left[\hat{\mathbf{H}}^{\mathrm{cb}}_{k,\ell+\Delta_\ell}\right]_{i,j} = \tau^{\mathrm{cb}}_k(\Delta_\ell)\frac{\beta^{\mathrm{cb}}_k\left[\mathbf{\Omega}^{\mathrm{cb}}_k\right]_{i,j}}{\sum_{k'=0}^{K-1}\beta^{\mathrm{cb}}_{k'}\left[\mathbf{\Omega}^{\mathrm{cb},\phi_{k'}-\phi_k}_{k'}\right]_{i,j}+\sum_{d'=0}^{D-1}\beta^{\mathrm{vb}}_{d'}\left[\mathbf{\Omega}^{\mathrm{vb},\phi_{d'}-\phi_k}_{d'}\right]_{i,j}+\frac{\sigma_{\mathrm{z}}}{\sigma_{\mathrm{t}}}}\left[\mathbf{Y}^{\mathrm{b}}_{k,\ell}\right]_{i,j}$$

$$\left[\hat{\mathbf{H}}^{\mathrm{vv}}_{d,d,\ell+\Delta_\ell}\right]_{i,j} = \tau^{\mathrm{vv}}_{d,d}(\Delta_\ell)\frac{\beta^{\mathrm{vv}}_{d,d}\left[\mathbf{\Omega}^{\mathrm{vv}}_{d,d}\right]_{i,j}}{\sum_{d'=0}^{D-1}\beta^{\mathrm{vv}}_{d',d}\left[\mathbf{\Omega}^{\mathrm{vv},\phi_{d'}-\phi_d}_{d',d}\right]_{i,j}+\sum_{k'=0}^{K-1}\beta^{\mathrm{cv}}_{k',d}\left[\mathbf{\Omega}^{\mathrm{cv},\phi_{k'}-\phi_d}_{k',d}\right]_{i,j}+\frac{\sigma_{\mathrm{z}}}{\sigma_{\mathrm{t}}}}\left[\mathbf{Y}^{\mathrm{v}}_{d,d,\ell}\right]_{i,j} \tag{23}$$

$$\begin{aligned}\epsilon^{\mathrm{b,CP}}(\Delta_\ell) &\triangleq \sum_{k=0}^{K-1}\sum_{i=0}^{M-1}\sum_{j=0}^{N_{\mathrm{g}}-1}\mathrm{E}\left\{\left|\left[\mathbf{H}^{\mathrm{cb}}_{k,\ell+\Delta_\ell}-\hat{\mathbf{H}}^{\mathrm{cb}}_{k,\ell+\Delta_\ell}\right]_{i,j}\right|^2\right\}\\ &= \sum_{k=0}^{K-1}\sum_{i=0}^{M-1}\sum_{j=0}^{N_{\mathrm{g}}-1}\left\{\beta^{\mathrm{cb}}_k\left[\mathbf{\Omega}^{\mathrm{cb}}_k\right]_{i,j}-\left[\beta^{\mathrm{cb}}_k\tau^{\mathrm{cb}}_k(\Delta_\ell)\right]^2\cdot\frac{\left[\mathbf{\Omega}^{\mathrm{cb}}_k\right]^2_{i,j}}{\sum_{k'=0}^{K-1}\beta^{\mathrm{cb}}_{k'}\left[\mathbf{\Omega}^{\mathrm{cb},\phi_{k'}-\phi_k}_{k'}\right]_{i,j}+\sum_{d'=0}^{D-1}\beta^{\mathrm{vb}}_{d'}\left[\mathbf{\Omega}^{\mathrm{vb},\phi_{d'}-\phi_k}_{d'}\right]_{i,j}+\frac{\sigma_{\mathrm{ztr}}}{\sigma_{\mathrm{xtr}}}}\right\}\\ \epsilon^{\mathrm{v,CP}}(\Delta_\ell) &\triangleq \sum_{d=0}^{D-1}\sum_{i=0}^{N_d-1}\sum_{j=0}^{N_{\mathrm{g}}-1}\mathrm{E}\left\{\left|\left[\mathbf{H}^{\mathrm{vv}}_{d,d,\ell+\Delta_\ell}-\hat{\mathbf{H}}^{\mathrm{vv}}_{d,d,\ell+\Delta_\ell}\right]_{i,j}\right|^2\right\}\\ &= \sum_{k=0}^{K-1}\sum_{i=0}^{N_d-1}\sum_{j=0}^{N_{\mathrm{g}}-1}\left\{\beta^{\mathrm{vv}}_{d,d}\left[\mathbf{\Omega}^{\mathrm{vv}}_{d,d}\right]_{i,j}-\left[\beta^{\mathrm{vv}}_{d,d}\tau^{\mathrm{vv}}_{d,d}(\Delta_\ell)\right]^2\cdot\frac{\left[\mathbf{\Omega}^{\mathrm{vv}}_{d,d}\right]^2_{i,j}}{\sum_{d'=0}^{D-1}\beta^{\mathrm{vv}}_{d',d}\left[\mathbf{\Omega}^{\mathrm{vv},\phi_{d'}-\phi_d}_{d',d}\right]_{i,j}+\sum_{k'=0}^{K-1}\beta^{\mathrm{cv}}_{k',d}\left[\mathbf{\Omega}^{\mathrm{cv},\phi_{k'}-\phi_d}_{k',d}\right]_{i,j}+\frac{\sigma_{\mathrm{ztr}}}{\sigma_{\mathrm{xtr}}}}\right\}\end{aligned} \tag{25}$$

Algorithm 1 AD Domain Channel Power Spectrum Based Pilot Allocation (ADCPS-PA) Algorithm

Input: γ, $\mathcal{K}$, $\mathcal{V}_{\mathrm{Tx}}$, $\mathcal{V}_{\mathrm{Rx}}$, $\left\{\mathbf{\Omega}_i^{\mathrm{xb}} : i \in \mathcal{K} \cup \mathcal{V}_{\mathrm{Tx}}, \mathrm{x} \in \{\mathrm{c}, \mathrm{v}\}\right\}$, $\left\{\mathbf{\Omega}_{i,j}^{\mathrm{xv}} : i \in \mathcal{K} \cup \mathcal{V}_{\mathrm{Tx}}, j \in \mathcal{V}_{\mathrm{Rx}}, \mathrm{x} \in \{\mathrm{c}, \mathrm{v}\}\right\}$, $\left\{\beta_i^{\mathrm{xb}} : i \in \mathcal{K} \cup \mathcal{V}_{\mathrm{Tx}}, \mathrm{x} \in \{\mathrm{c}, \mathrm{v}\}\right\}$, $\left\{\beta_{i,j}^{\mathrm{xv}} : i \in \mathcal{K} \cup \mathcal{V}_{\mathrm{Tx}}, j \in \mathcal{V}_{\mathrm{Rx}}, \mathrm{x} \in \{\mathrm{c}, \mathrm{v}\}\right\}$,

Output: $\{\phi_i : i \in \mathcal{T}, \mathcal{T} = \mathcal{K} \cup \mathcal{V}_{\mathrm{Tx}}\}$

1: Initialization: $\mathcal{T} = \mathcal{K} \cup \mathcal{V}_{\mathrm{Tx}}$, $\phi_0 = 0$, $\mathcal{T}^{\mathrm{sch}} = \{0\}$, $\mathcal{T}^{\mathrm{un}} = \mathcal{T} \backslash \mathcal{T}^{\mathrm{sch}}$
2: **while** $\mathcal{T}^{\mathrm{un}} \neq \varnothing$ **do**
3: For $i \in \mathcal{T}^{\mathrm{un}}$, find a phase shift ϕ from the available phase shifts $0, 1, \ldots$ in sequence which firstly satisfies $\mathrm{DR}\left(\{i\}, \mathcal{T}^{\mathrm{sch}}\right) \leq \gamma$
4: If ϕ cannot be obtained via step 3, then $\phi = \arg\min \mathrm{DR}\left(\{i\}, \mathcal{T}^{\mathrm{sch}}\right)$
5: Update: $\phi_i = \phi$, $\mathcal{T}^{\mathrm{sch}} \leftarrow \mathcal{T}^{\mathrm{sch}} \cup \{i\}$, $\mathcal{T}^{\mathrm{un}} \leftarrow \mathcal{T}^{\mathrm{un}} \backslash \{i\}$
6: **end while**

which has been widely adopted in previous works such as [8], [12], [16]. Assume that a ULA with half wavelength spacing antennas is considered at the BS and the VRxs, and the major parameters for the V2V underlay mMIMO-OFDM are set as follows: $M = 128$, $N_d = 64$, $K = D = 21$, $N_{\mathrm{c}} = 2048$, $N_{\mathrm{g}} = 144$, $T_{\mathrm{s}} = 32.6$ ns, and the system bandwidth is 20 MHz.

With the above settings, the OFDM symbol length of the pilot segment for the conventional PSOP approach is given by $\lceil (K+D)N_{\mathrm{g}}/N_{\mathrm{c}} \rceil = 3$ [17]. Meanwhile, the pilot length for the proposed PSAP approach is set as 1 symbol. Assume that a frame consists of 7 OFDM symbols, where the first part is set to be the pilot segment and the following symbols are utilized for the uplink data segment and the downlink data segment, both occupying half of the data segment.

We consider channels with an exponential power delay profile and a Laplacian power angle spectrum in each tap [8]. Assume that uniform distributions are employed for the mean angles of arrival and the locations of all the CUs and VTxs. The large-scale fading coefficient can be obtained by $\beta = d^{-\alpha}$ for all links, where d is the distance between the transmitter and the receiver and α denotes the path-loss propagation exponent. Set $\beta_i^{\mathrm{xb}} = 120^{-4.37}$ and $\beta_{i,d}^{\mathrm{xv}} = 50^{-3.76}$ for $\mathrm{x} \in \{\mathrm{c}, \mathrm{v}\}$, $i \in \mathcal{K} \cup \mathcal{V}_{\mathrm{Tx}}$, and $d \in \mathcal{V}_{\mathrm{Rx}}$. Assume that the transmit power during the pilot segment and the data segment are equal, and the noise power is set as -105 dBm.

Assume that the Doppler, delay, and angle spread are same for all the CUs and VTxs. Two typical mobility scenarios are considered: urban macro (UMa) scenario (doppler is 1.4×10^{-2}, delay spread is 1.85 μs, angle spread is 2°, velocity is 100 km/h), and urban micro (UMi) scenario (doppler is 6.6×10^{-3}, delay spread is 0.62 μs, angle spread is 10°, velocity is 50 km/h). Besides, Algorithm 1 is adopted to perform pilot allocation and the threshold is set as $\gamma = 10^{-7}$ in the simulations.

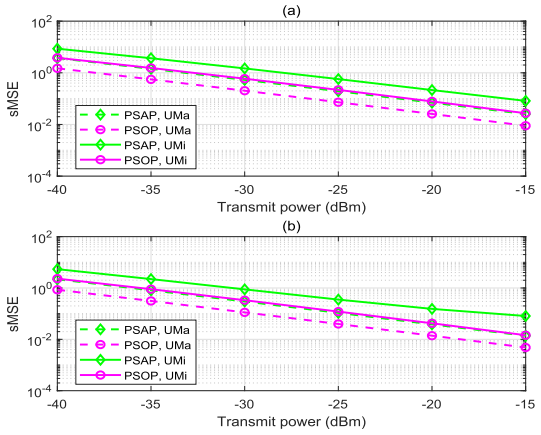

FIGURE 2. The pilot segment sMSE performance of the proposed PSAPs and the conventional PSOPs under the UMa and UMi scenario. (a) Cellular links; (b) V2V links.

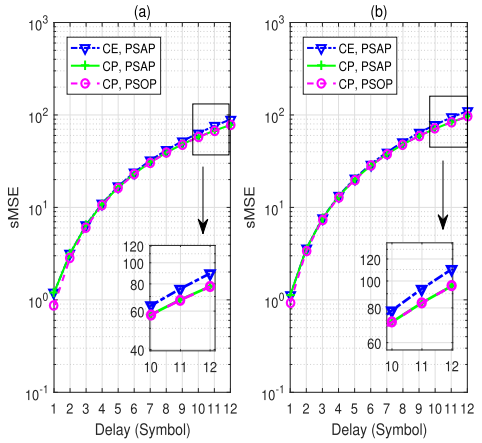

FIGURE 3. The data segment sMSE performance of the proposed PSAPs and the conventional PSOPs under the UMa scenario with $\sigma_t = -30$ dBm. (a) Cellular links; (b) V2V links.

In Fig. 2, we plot the sMSE performance in pilot segment obtained by the proposed PSAPs and the conventional PSOPs under UMa and UMi scenarios. It can be observed that for both cellular and V2V links, CE performance with the PSAPs is comparable to that obtained by the PSOP approach in both the considered scenarios, while the pilot overhead is decreased by 66.7%.

Fig. 3 and Fig. 4 present the sMSE performance during data segment versus the delay between the data symbol and pilot segment with $\sigma_t = -30$ dBm under UMa scenario and UMi scenario, respectively. We can see that CP achieves better performance than CE with PSAPs, especially when the delay Δ_ℓ increases. Besides, there is not much difference between the CP performance obtained via the PSAPs and the PSOPs in both scenarios, whereas pilot overhead for PSAPs is only 33.7% of that for PSOPs.

Consider an MMSE receiver for the uplink data segment and an MMSE precoder for the downlink data segment. In Fig. 5, we compare the achievable spectral efficiency with

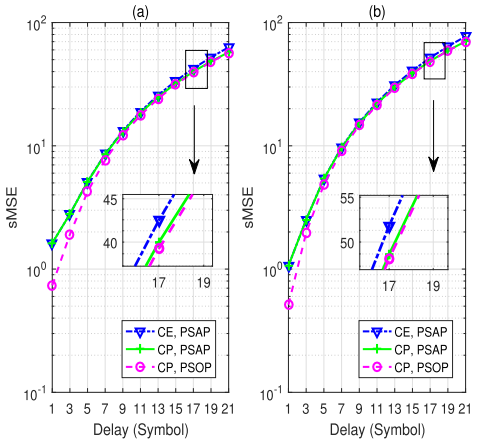

FIGURE 4. The data segment sMSE performance of the proposed PSAPs and the conventional PSOPs under the UMi scenario with $\sigma_t = -30$ dBm. (a) Cellular links; (b) V2V links.

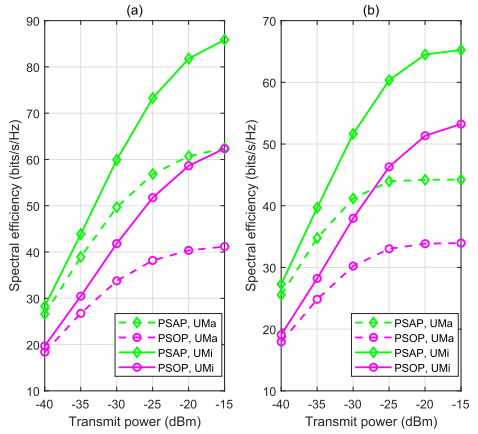

FIGURE 5. The achievable spectral efficiency performances of the proposed PSAPs and the conventional PSOPs under the UMa and UMi scenario. (a) Cellular links. (b) V2V links.

PSAPs and PSOPs under the UMa scenario and the UMi scenario. From Fig. 5, we can see that the spectral efficiency performances are dramatically improved with PSAPs for both cellular and V2V links, compared with those obtained by the conventional PSOPs. Note that the performance boost is more significant at high transmit power where the PI is dominant and high mobility where the pilot overhead is dominant. Especially, with a transmit power of -15 dBm, the proposed PSAP approach provides about 37.7 % and 22.6 % achievable spectral efficiency increase for the cellular and V2V communications respectively over the conventional PSOP approach under the UMi scenario, whereas the performance gains are about 51.6 % and 30.3 % for the cellular and V2V links respectively under the UMa scenario with the same transmit power.

VII. CONCLUSION

In this paper, PSAPs were proposed for the channel acquisition in V2V underlay mMIMO-OFDM communication for the pilot overhead reduction and the spectral efficiency improvement. According to the channel sparse property in the AD domain, We investigated channel estimation in the pilot segment and channel prediction in the data segment with the proposed PSAPs, and derived the optimal conditions to achieve the minimum sMSEs. Then according to the optimal conditions, we developed an ADCPS-PA algorithm. Simulation results showed that significantly enhanced spectral efficiency can be obtained by the proposed PSAPs compared with the PSOPs for both CUs and V2V communication pairs.

APPENDIX A
PROOF OF PROPOSITION 1

Based on the definition for $\mathbf{\Omega}_{k'}^{\mathrm{cb},\phi_{k'}-\phi_k}$ and $\mathbf{\Omega}_{d'}^{\mathrm{vb},\phi_{d'}-\phi_k}$, we can know that the elements of these matrices are all non-negative. Thus, the minimum value of $\epsilon^{\mathrm{b,CE}}$ can be readily obtained as shown in (32) at the top of the next page.

If the condition $\left(\bar{\mathbf{\Omega}}_{k,(N_\mathrm{c})}^{\mathrm{cb}}\mathbf{\Pi}_{N_\mathrm{c}}^{\phi_k}\right)\odot\left(\bar{\mathbf{\Omega}}_{k',(N_\mathrm{c})}^{\mathrm{cb}}\mathbf{\Pi}_{N_\mathrm{c}}^{\phi_{k'}}\right) = \left(\bar{\mathbf{\Omega}}_{k,(N_\mathrm{c})}^{\mathrm{cb}}\mathbf{\Pi}_{N_\mathrm{c}}^{\phi_k}\right)\odot\left(\bar{\mathbf{\Omega}}_{d',(N_\mathrm{c})}^{\mathrm{vb}}\mathbf{\Pi}_{N_\mathrm{c}}^{\phi_{d'}}\right) = \mathbf{0}$ is met, after performing the same column permutation and column truncation for these matrices, it is obvious that

$$\begin{aligned}&\left(\bar{\mathbf{\Omega}}_{k,(N_\mathrm{c})}^{\mathrm{cb}}\mathbf{\Pi}_{N_\mathrm{c}}^{\phi_k}\mathbf{\Pi}_{N_\mathrm{c}}^{-\phi_k}\mathbf{I}_{N_\mathrm{c}\times N_\mathrm{g}}\right)\odot\left(\bar{\mathbf{\Omega}}_{k',(N_\mathrm{c})}^{\mathrm{cb}}\mathbf{\Pi}_{N_\mathrm{c}}^{\phi_{k'}}\mathbf{\Pi}_{N_\mathrm{c}}^{-\phi_k}\mathbf{I}_{N_\mathrm{c}\times N_\mathrm{g}}\right)\\&=\left(\bar{\mathbf{\Omega}}_{k,(N_\mathrm{c})}^{\mathrm{cb}}\mathbf{\Pi}_{N_\mathrm{c}}^{\phi_k}\mathbf{\Pi}_{N_\mathrm{c}}^{-\phi_k}\mathbf{I}_{N_\mathrm{c}\times N_\mathrm{g}}\right)\odot\left(\bar{\mathbf{\Omega}}_{d',(N_\mathrm{c})}^{\mathrm{vb}}\mathbf{\Pi}_{N_\mathrm{c}}^{\phi_{d'}}\mathbf{\Pi}_{N_\mathrm{c}}^{-\phi_k}\mathbf{I}_{N_\mathrm{c}\times N_\mathrm{g}}\right)\\&=\mathbf{0}.\end{aligned}\tag{33}$$

Obviously the permutation matrix satisfies the following property

$$\mathbf{\Pi}_N^a\mathbf{\Pi}_N^b=\mathbf{\Pi}_N^{a+b}.\tag{34}$$

Then from (14) and (34), we can see that

$$\begin{aligned}\bar{\mathbf{\Omega}}_{k,(N_\mathrm{c})}^{\mathrm{cb}}\mathbf{\Pi}_{N_\mathrm{c}}^{\phi_k}\mathbf{\Pi}_{N_\mathrm{c}}^{-\phi_k}\mathbf{I}_{N_\mathrm{c}\times N_\mathrm{g}}&=\mathbf{\Omega}_k^{\mathrm{cb}},\\\bar{\mathbf{\Omega}}_{k',(N_\mathrm{c})}^{\mathrm{cb}}\mathbf{\Pi}_{N_\mathrm{c}}^{\phi_{k'}}\mathbf{\Pi}_{N_\mathrm{c}}^{-\phi_k}\mathbf{I}_{N_\mathrm{c}\times N_\mathrm{g}}&=\mathbf{\Omega}_{k'}^{\mathrm{cb},\phi_{k'}-\phi_k},\end{aligned}\tag{35}$$

and similarly,

$$\bar{\mathbf{\Omega}}_{d',(N_\mathrm{c})}^{\mathrm{vb}}\mathbf{\Pi}_{N_\mathrm{c}}^{\phi_{d'}}\mathbf{\Pi}_{N_\mathrm{c}}^{-\phi_k}\mathbf{I}_{N_\mathrm{c}\times N_\mathrm{g}}=\mathbf{\Omega}_{d'}^{\mathrm{vb},\phi_{d'}-\phi_k}.\tag{36}$$

Thus, the condition in (33) is equivalent to

$$\mathbf{\Omega}_k^{\mathrm{cb}}\odot\mathbf{\Omega}_{k'}^{\mathrm{cb},\phi_{k'}-\phi_k}=\mathbf{\Omega}_k^{\mathrm{cb}}\odot\mathbf{\Omega}_{d'}^{\mathrm{vb},\phi_{d'}-\phi_k}=\mathbf{0}.\tag{37}$$

Then for $\forall k\neq k'\in\mathcal{K}$ and $\forall d'\in\mathcal{V}_{\mathrm{Tx}}$, (38), as shown at the top of the next page, can be obtained, leading to (39), as shown at the top of the next page. Substituting (39) to (16), we get

$$\begin{aligned}\varepsilon^{\mathrm{b,CE}}&=\sum_{k=0}^{K-1}\varepsilon_k^{\mathrm{cb,CE}}\\&=\sum_{k=0}^{K-1}\sum_{i=0}^{M-1}\sum_{j=0}^{N_\mathrm{g}-1}\left\{\beta_k^{\mathrm{cb}}\left[\mathbf{\Omega}_k^{\mathrm{cb}}\right]_{i,j}-\frac{(\beta_k^{\mathrm{cb}})^2\left[\mathbf{\Omega}_k^{\mathrm{cb}}\right]_{i,j}^2}{\beta_k^{\mathrm{cb}}\left[\mathbf{\Omega}_k^{\mathrm{cb}}\right]_{i,j}+\frac{\sigma_z}{\sigma_t}}\right\},\end{aligned}\tag{40}$$

i.e., the minimum of the sMSE $\epsilon^{\mathrm{b,CE}}$ is achieved.

$$\epsilon^{\mathrm{b,CE}} = \sum_{k=0}^{K-1}\sum_{i=0}^{M-1}\sum_{j=0}^{N_{\mathrm{g}}-1}\left\{\beta_k^{\mathrm{cb}}\left[\boldsymbol{\Omega}_k^{\mathrm{cb}}\right]_{i,j} - \frac{(\beta_k^{\mathrm{cb}})^2\left[\boldsymbol{\Omega}_k^{\mathrm{cb}}\right]_{i,j}^2}{\sum_{k'=0}^{K-1}\beta_{k'}^{\mathrm{cb}}\left[\boldsymbol{\Omega}_{k'}^{\mathrm{cb},\phi_{k'}-\phi_k}\right]_{i,j} + \sum_{d'=0}^{D-1}\beta_{d'}^{\mathrm{vb}}\left[\boldsymbol{\Omega}_{d'}^{\mathrm{vb},\phi_{d'}-\phi_k}\right]_{i,j} + \frac{\sigma_{\mathrm{z}}}{\sigma_{\mathrm{t}}}}\right\}$$
$$\geq \sum_{k=0}^{K-1}\sum_{i=0}^{M-1}\sum_{j=0}^{N_{\mathrm{g}}-1}\left\{\beta_k^{\mathrm{cb}}\left[\boldsymbol{\Omega}_k^{\mathrm{cb}}\right]_{i,j} - \frac{(\beta_k^{\mathrm{cb}})^2\left[\boldsymbol{\Omega}_k^{\mathrm{cb}}\right]_{i,j}^2}{\beta_k^{\mathrm{cb}}\left[\boldsymbol{\Omega}_k^{\mathrm{cb}}\right]_{i,j} + \frac{\sigma_{\mathrm{z}}}{\sigma_{\mathrm{t}}}}\right\} = \varepsilon^{\mathrm{b,CE}} \tag{32}$$

$$\left[\boldsymbol{\Omega}_k^{\mathrm{cb}}\right]_{i,j}^2\left\{\beta_k^{\mathrm{cb}}\left[\boldsymbol{\Omega}_k^{\mathrm{cb}}\right]_{i,j} + \sum_{k'\neq k}\beta_{k'}^{\mathrm{cb}}\left[\boldsymbol{\Omega}_{k'}^{\mathrm{cb},\phi_{k'}-\phi_k}\right]_{i,j} + \sum_{d'=0}^{D-1}\beta_{d'}^{\mathrm{vb}}\left[\boldsymbol{\Omega}_{d'}^{\mathrm{vb},\phi_{d'}-\phi_k}\right]_{i,j} + \frac{\sigma_{\mathrm{z}}}{\sigma_{\mathrm{t}}}\right\} = \left[\boldsymbol{\Omega}_k^{\mathrm{cb}}\right]_{i,j}^2\left\{\beta_k^{\mathrm{cb}}\left[\boldsymbol{\Omega}_k^{\mathrm{cb}}\right]_{i,j} + \frac{\sigma_{\mathrm{z}}}{\sigma_{\mathrm{t}}}\right\} \tag{38}$$

$$\frac{\left[\boldsymbol{\Omega}_k^{\mathrm{cb}}\right]_{i,j}^2}{\beta_k^{\mathrm{cb}}\left[\boldsymbol{\Omega}_k^{\mathrm{cb}}\right]_{i,j} + \sum_{k'\neq k}\beta_{k'}^{\mathrm{cb}}\left[\boldsymbol{\Omega}_{k'}^{\mathrm{cb},\phi_{k'}-\phi_k}\right]_{i,j} + \sum_{d'=0}^{D-1}\beta_{d'}^{\mathrm{vb}}\left[\boldsymbol{\Omega}_{d'}^{\mathrm{vb},\phi_{d'}-\phi_k}\right]_{i,j} + \frac{\sigma_{\mathrm{z}}}{\sigma_{\mathrm{t}}}} = \frac{\left[\boldsymbol{\Omega}_k^{\mathrm{cb}}\right]_{i,j}^2}{\beta_k^{\mathrm{cb}}\left[\boldsymbol{\Omega}_k^{\mathrm{cb}}\right]_{i,j} + \frac{\sigma_{\mathrm{z}}}{\sigma_{\mathrm{t}}}} \tag{39}$$

In addition, due to the fact that the elements of $\boldsymbol{\Omega}_{k',d}^{\mathrm{cv},\phi_{k'}-\phi_d}$ and $\boldsymbol{\Omega}_{d',d}^{\mathrm{vv},\phi_{v'}-\phi_k}$ are non-negative, the minimum value of $\epsilon^{\mathrm{v,CE}}$ and the corresponding optimal condition to achieve the minimum can be derived utilizing the same methodology as presented above.

This concludes the proof.

REFERENCES

[1] R. Molina-Masegosa and J. Gozalvez, "LTE-V for sidelink 5G V2X vehicular communications: A new 5G technology for short-range Vehicle-to-Everything communications," *IEEE Veh. Technol. Mag.*, vol. 12, no. 4, pp. 30–39, Dec. 2017.

[2] F. Abbas, P. Fan, and Z. Khan, "A novel low-latency V2 V resource allocation scheme based on cellular V2X communications," *IEEE Trans. Intell. Transp. Syst.*, vol. 20, no. 6, pp. 2185–2197, Jun. 2019.

[3] X. Liu, Y. Li, L. Xiao, and J. Wang, "Performance analysis and power control for multi-antenna V2 V underlay massive MIMO," *IEEE Trans. Wireless Commun.*, vol. 17, no. 7, pp. 4374–4387, Jul. 2018.

[4] H. Jiang, Z. Zhang, J. Dang, and L. Wu, "A novel 3-D massive MIMO channel model for Vehicle-to-Vehicle communication environments," *IEEE Trans. Commun.*, vol. 66, no. 1, pp. 79–90, Jan. 2018.

[5] H. Jiang, W. Ying, J. Zhou, and G. Shao, "A 3D wideband two-cluster channel model for massive MIMO Vehicle-to-Vehicle communications in semi-ellipsoid environments," *IEEE Access*, vol. 8, pp. 23594–23600, 2020.

[6] N. N. Tran, H. H. Nguyen, H. D. Tuan, and D. E. Dodds, "Training signal designs for spatially correlated multi-user multi-input multi-output with orthogonal frequency-division multiplexing systems," *IET Commun.*, vol. 6, no. 16, pp. 2630–2638, Nov. 2012.

[7] L. You, X. Gao, X.-G. Xia, N. Ma, and Y. Peng, "Pilot reuse for massive MIMO transmission over spatially correlated Rayleigh fading channels," *IEEE Trans. Wireless Commun.*, vol. 14, no. 6, pp. 3352–3366, Jun. 2015.

[8] L. You, X. Gao, A. L. Swindlehurst, and W. Zhong, "Channel acquisition for massive MIMO-OFDM with adjustable phase shift pilots," *IEEE Trans. Signal Process.*, vol. 64, no. 6, pp. 1461–1476, Mar. 2016.

[9] C. Pan, H. Mehrpouyan, Y. Liu, M. Elkashlan, and N. Arumugam, "Joint pilot allocation and robust transmission design for ultra-dense user-centric TDD C-RAN with imperfect CSI," *IEEE Trans. Wireless Commun.*, vol. 17, no. 3, pp. 2038–2053, Mar. 2018.

[10] H. Xu, W. Xu, Z. Yang, J. Shi, and M. Chen, "Pilot reuse among D2D users in D2D underlaid massive MIMO systems," *IEEE Trans. Veh. Technol.*, vol. 67, no. 1, pp. 467–482, Jan. 2018.

[11] H. Echigo and T. Ohtsuki, "Graph coloring-based pilot reuse with AOA and distance in D2D underlay massive MIMO," in *Proc. IEEE 87th Veh. Technol. Conf. (VTC Spring)*, Jun. 2018, pp. 1–6.

[12] L. You, M. Xiao, X. Song, Y. Liu, W. Wang, X. Gao, and G. Fettweis, "Pilot reuse for Vehicle-to-Vehicle underlay massive MIMO transmission," *IEEE Trans. Veh. Technol.*, vol. 69, no. 5, pp. 5693–5697, May 2020.

[13] Z. Chen and C. Yang, "Pilot decontamination in wideband massive MIMO systems by exploiting channel sparsity," *IEEE Trans. Wireless Commun.*, vol. 15, no. 7, pp. 5087–5100, Jul. 2016.

[14] Q. Qin, L. Gui, B. Gong, and S. Luo, "Sparse channel estimation for massive MIMO-OFDM systems over time-varying channels," *IEEE Access*, vol. 6, pp. 33740–33751, 2018.

[15] J. Mo, P. Schniter, and R. W. Heath, "Channel estimation in broadband millimeter wave MIMO systems with few-bit ADCs," *IEEE Trans. Signal Process.*, vol. 66, no. 5, pp. 1141–1154, Mar. 2018.

[16] C.-K. Wen, S. Jin, K.-K. Wong, J.-C. Chen, and P. Ting, "Channel estimation for massive MIMO using Gaussian-mixture Bayesian learning," *IEEE Trans. Wireless Commun.*, vol. 14, no. 3, pp. 1356–1368, Mar. 2015.

[17] T. L. Marzetta, "Noncooperative cellular wireless with unlimited numbers of base station antennas," *IEEE Trans. Wireless Commun.*, vol. 9, no. 11, pp. 3590–3600, Nov. 2010.

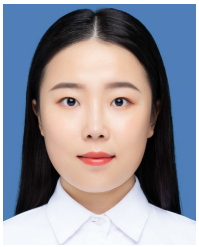

XINXIN NIU (Student Member, IEEE) received the B.E. degree in electrical engineering from Southeast University, Nanjing, China, in 2014, where she is currently pursuing the Ph.D. degree with the National Mobile Communications Research Laboratory. Her research interests include massive MIMO communications and signal processing.

LI YOU (Member, IEEE) received the B.E. and M.E. degrees in electrical engineering from the Nanjing University of Aeronautics and Astronautics, Nanjing, China, in 2009 and 2012, respectively, and the Ph.D. degree in electrical engineering from Southeast University, Nanjing, in 2016.

From September 2014 to September 2015, he conducted visiting research with the Center for Pervasive Communications and Computing, University of California at Irvine, Irvine, CA, USA. Since 2016, he has been with the Faculty of the National Mobile Communications Research Laboratory, Southeast University. His current research interests include communications, signal processing, and information theory, with emphasis on massive MIMO communications.

XIQI GAO (Fellow, IEEE) received the Ph.D. degree in electrical engineering from Southeast University, Nanjing, China, in 1997.

He joined the Department of Radio Engineering, Southeast University, in 1992, where he has been a Professor of information systems and communications, since 2001. From 1999 to 2000, he was a Visiting Scholar with the Massachusetts Institute of Technology, Cambridge, MA, USA, and Boston University, Boston, MA, USA. From 2007 to 2008, he was a Humboldt Scholar with the Darmstadt University of Technology, Darmstadt, Germany. His current research interests include broadband multicarrier communications, MIMO wireless communications, channel estimation and turbo equalization, and multirate signal processing for wireless communications.

Dr. Gao received the Science and Technology Awards of the State Education Ministry of China, in 1998, 2006, and 2009, the National Technological Invention Award of China, in 2011, and the 2011 IEEE Communications Society Stephen O. Rice Prize Paper Award in communications theory.